Journal of Materials Chemistry

Cite this: *J. Mater. Chem.*, 2012, **22**, 14861

www.rsc.org/materials

COMMUNICATION

Rapid and shape-controlled synthesis of "clean" star-like and concave Pd nanocrystallites and their high performance toward methanol oxidation†

Yu-Ling Qin,[ab] Xin-Bo Zhang,*[a] Jun Wang[a] and Li-Min Wang*[a]

Received 9th March 2012, Accepted 20th June 2012
DOI: 10.1039/c2jm32682e

Uniform "clean" star-shaped and concave palladium (Pd) nanocrystallites (NCs) are first successfully synthesized *via* a very simple and rapid route without using any surfactants. Interestingly, the as-prepared Pd NCs manifest superior electrocatalytic activity and stability toward methanol oxidation over the commercial Pd/C catalyst.

Platinum-group metals (PGMs), including platinum (Pt) and palladium (Pd), are excellent and versatile catalysts in various important reactions.[1] Compared to Pt, Pd has a much higher abundance in nature[2] and better resistance to carbon monoxide (CO)[3] and thus is employed as a very important electrocatalyst in direct methanol fuel cells (DMFCs). However, the state-of-the-art Pd catalysts are still unable to meet the challenge of the ever-increasing performance demand of DMFCs.[4] Nanostructured materials show unique shape- and/or size-dependent chemical and physical properties that drastically differ from their bulky counterparts.[5] Therefore, further enhancement of the catalytic performance by tuning the morphology of Pd NCs is of great fundamental importance.[6] So far, Pd NCs with diverse shapes, such as cubes, plates, rods, bars *etc.*, have been successfully synthesized.[7] However, to get uniform Pd NCs, most of the synthetic methods reported to date rely heavily on organic solvents and/or surfactants and/or extremely long and prudent operations, which are uneconomic, ungreen, and unfavourable for practical applications.[8] What's worse, the surfactants would inevitably poison the sample surface which is vital for applications such as catalysts.[2a] Consequently, additional thermal and oxidative approaches are indispensable to "clean" the catalyst, which not only complicates the synthesis process, but also leads to unwanted size and shape changes, and especially is highly reproducible.[9] Therefore, the development of a mild, template- and surfactant-free strategy for the one-step controllable synthesis of "clean" Pd NCs in aqueous solution and for further discovering their intrinsically catalytic activities is highly desirable and technologically important.

Herein, we propose a very simple and rapid strategy to synthesize Pd nanostars (NSs) and concave nanoparticles (CNs) by reducing tetrachloropalladinic acid (H_2PdCl_4) in only 5 minutes at room temperature in aqueous solution, wherein neither surfactants nor dispersion agents are employed. Also, the pH value of the solution plays a key role in tuning the shape of the Pd NSs and CNs. Surprisingly, the as-synthesized Pd NCs possess a definitely "clean" surface and thus exert superior catalytic activity and stability toward methanol oxidation over the commercial Pd/C catalyst.

The synthetic procedures are schematically illustrated in Fig. 1. Briefly, Pd NSs are easily generated as a black suspension upon adding L-ascorbic acid (AA) to an aqueous solution of H_2PdCl_4 and potassium bromide (KBr) with vigorous shaking and then left undisturbed for 5 minutes. Interestingly, the CNs can be synthesized only by adding a small amount of sodium hydroxide (NaOH) into the precursor mixture before adding AA. The details of the synthetic procedure are given in the ESI.†

The morphology and structure of the as-synthesized samples are characterized by scanning electron microscopy (SEM) and transmission electron microscopy (TEM). Fig. 2A reveals that the resultant product is definitely endowed with star-like morphology with uniform size (*ca.* 250 nm), demonstrating the high yield of Pd NSs. These Pd NSs are further characterized by the TEM image (Fig. 2C) which shows that the cusp of the Pd NSs holds the symmetrical branching pattern shape. Fig. 2B and D show the SEM and TEM images of the Pd CNs (*ca.* 50 nm). It can be easily seen that the central part of the Pd CNs is darker than the edges, implying the formation of a concave structure rather than a plane on the surface of the NCs.[7a]

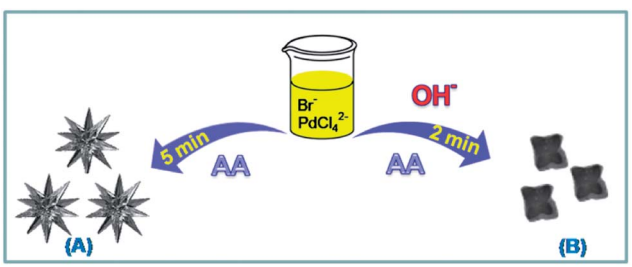

Fig. 1 Schematic illustration of synthesis processes for Pd NSs (A) and CNs (B).

[a]*State Key Laboratory of Rare Earth Resource Utilization, Changchun Institute of Applied Chemistry, Chinese Academy of Sciences, Changchun 130022, Jilin, China. E-mail: xbzhang@ciac.jl.cn; lmwang@ciac.jl.cn; Fax: +86 431-85262235; Tel: +86 431-85262235*
[b]*Graduate School of the Chinese Academy of Sciences, Beijing 100049, China*

† Electronic supplementary information (ESI) available: detailed synthesis conditions; experimental procedures; electron microscope characterization of Pd NCs; XRD characterization; XPS characterization; FT-IR characterization; CO stripping experiments; the cycle stability tests; CA curves. See DOI: 10.1039/c2jm32682e

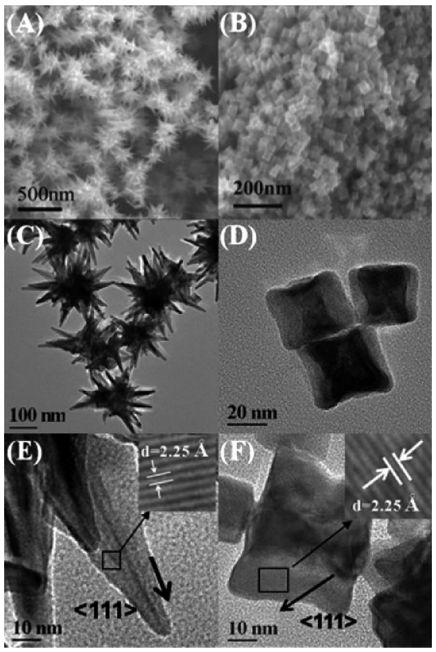

Fig. 2 SEM (A and B), TEM (C and D) and HRTEM (E and F) images of Pd NSs (left) and Pd CNs (right).

As is shown in the high-resolution TEM (HRTEM) images (Fig. 2E and F), the crystallographic alignment of both the NSs and CNs reveals a lattice spacing of 0.225 nm, indicating that the Pd nanoparticles grow along the <111> direction. The X-ray diffraction (XRD) patterns demonstrate that the peaks of both nanoparticles can be referenced to a face-centered cubic unit cell with the lattice constant $a = 3.89$ Å (Fig. S1†). The 2θ values of 40.12°, 46.66°, and 68.12° can be indexed to diffractions of the (111), (200), and (220) planes, respectively (PDF#46-1043). These characters would affect their catalytic active performance. However, star-like Pd NCs cannot be formed directly on the carbon support (Fig. S2A†).

In order to elucidate the mechanism involved in the formation of Pd NCs, different control experiments are performed by changing the concentrations of the reagents used, including NaOH, H_2PdCl_4, KBr, and AA. It is found that the shape of the formed Pd NCs is highly sensitive to the concentrations of these reagents (Fig. S3 and S4†). For example, with the increase in pH value, the number of CNs increases at the expense of the decrease in NSs (Fig. S3A–C†). Until the pH value reaches 3.16 (added 1.1 mL of NaOH), the Pd NSs totally disappear (Fig. S3D†) and homogeneous Pd CNs are obtained. This is because the increase in pH would accelerate the reduction process and thus the concentration of metal atoms in the solution is increased. As a result, the fast generated atoms homogeneously deposit on the seeds rather than selectively adding to the edges and corners, resulting in the shape evolution from NSs to CNs. On the other hand, only severely aggregated Pd NSs can be obtained in the case of lower concentrations of KBr (Fig. S4A†) and/or $PdCl_4^{2-}$ (Fig. S4E†) or higher concentrations of AA (Fig. S4D†). In contrast, a higher concentration of KBr (Fig. S4B†) and/or $PdCl_4^{2-}$ (Fig. S4F†) or a lower concentration of AA (Fig. S4C†) is apt to form obtuse NSs. It is generally considered that the formation of NCs goes through nucleation and growth processes. Fast nucleation preferably results in numerous small particles (Fig. S4A, D, and E†), while a small quantity of big particles (Fig. S4B, C, and F†) will be obtained stemming from a faster growth process. As discussed by Chernov,[10] the growth habit of seeds depends on the diffusion rate (denoted by V_1) of the precursor from solution to the surface and the growth rate (denoted by V_2). Xia[7a] has discussed the relationship between V_1 and V_2 in detail. Herein, when V_1 is much smaller than V_2, a low concentration of metal atoms in the solution makes the atoms tend to add to the higher active sites of the nucleus rather than the entire surface,[11] resulting in sharp NSs forms. In contrast, when V_1 is much larger than V_2, atoms reduced from the precursor solution increase and add to different sites with equal probability, so it tends to form obtuse NSs. In particular, reducing the concentration of $PdCl_4^{2-}$ will slow down V_1, increasing the concentration of AA and reducing the concentration of KBr will speed up V_2. In addition, the growth rate of the {100} face will be retarded because Br^- can be selectively absorbed onto it, which further drives atoms to deposit at corners and edges. Thus, the formation of Pd NSs and CNs under the preparation conditions is understandable.

To gain insight into the morphological evolution of the Pd NSs, aliquots of the reaction solution are removed from the system at various reaction times and examined by TEM. Representative TEM images of the products sampled at 1, 2, 3, 4, 5, and 10 min are shown in Fig. S5.† At $t = 1$ min (Fig. S5A†), the product contains a large number of small Pd seeds (*ca.* 2 nm). In the following two minutes (Fig. S5B and C†), block-like NCs are observed. As the reaction proceeded to $t = 4$ min (Fig. S5D†), starfish-like NCs are found due to overgrowth on corners and edges. The mature Pd NSs are obtained until $t = 5$ min (Fig. S5E†), and further extending the reaction time (Fig. S5F†) results in no changes in the morphology and dimensions of the NSs. Fig. S5G† clearly presents the evolution from seeds to NSs, demonstrating that the as-prepared Pd NSs follow an overgrowth mode.

As no surfactant was employed during the whole synthesis process, "clean" NCs can be reasonably expected. To this end, Fourier transform infrared spectroscopy (FT-IR) and X-ray photoelectron spectrometry (XPS) are carried out. Compared to the strongly characterized peak of AA, no visible peak is observed from the sample in FT-IR, confirming the definitely "clean" surface of the obtained Pd NSs (Fig. S6†). Furthermore, the XPS results (Fig. S7†) show the absence of Br^- characteristic peaks, highlighting the power of the strategy in ensuring a clear surface of the Pd NSs.

Inspired by their "clean" surface, the Pd NSs/XC-72 (Fig. S2B†) and CNs/XC-72 (Fig. S2C†) are then evaluated as catalysts for the electro-oxidation of methanol. For comparison, a commercial Pd/C catalyst is employed as a benchmark material. The electrochemically active surface areas (ECSA) of both the Pd NCs and the commercial Pd/C catalyst are estimated by calculation of the CO desorption area from cyclic voltammograms (CV) in 0.5 M H_2SO_4 solution (Fig. S8†). Fig. 3 exhibits the CVs of Pd NCs and commercial Pd/C in 1 M methanol with 0.5 M NaOH. Apparently, methanol oxidation on Pd NSs/XC-72 starts at *ca.* −0.4 V and reaches the maximum current at −0.167 V, which is much lower than the onset voltage for commercial Pd/C (−0.082 V). The negative shift (0.085 V) of the oxidation potential indicates the enhanced electrocatalytic activity of the Pd NSs, implying an important advantage in increasing the working voltage of the fuel cells. Moreover, in the positive-going potential scan, the maximum current on Pd NSs/XC-72 is more than 3 times (as high as 336%) larger than that on the commercial Pd/C catalyst. During the reverse scan there is a secondary oxidation peak at −0.27 V, which is the same as for commercial Pd/C. Thus, we come

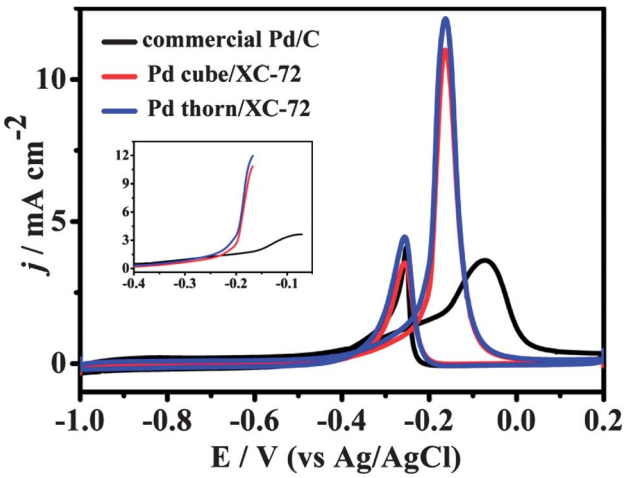

Fig. 3 Stable CV curves obtained for the Pd NCs/XC-72 and commercial Pd/C catalyst in an electrolyte of 0.5 M NaOH and 1 M CH_3OH at a scan rate of 50 mV s^{-1} at room temperature. Inset: CVs for methanol oxidation from −0.4 V to maximum in forward scan.

to the conclusion that our Pd NSs catalysts hold a higher catalytic activity toward electro-oxidation of methanol as well as its intermediate, CO. This is further supported by the CO stripping results (Fig. S8†) which show a negative shift of the CO oxidation peak potential (*ca.* 50 mV) for the Pd NS samples compared to the commercial Pd/C catalyst. Interestingly, the CV of the Pd CNs for methanol oxidation is nearly the same as that of the Pd NSs, only the maximum current is a little lower than the Pd NSs. This might be derived from their same growth direction and unit cell structure.

The stability is of great importance for the practical application of catalysts. There is no obvious decline for the Pd NSs and CNs in the electro-oxidation current after 100 potential scans (Fig. S9†), while the commercial Pd/C suffers a *ca.* 10% decline, indicating the superior stability of our catalysts. Moreover, the catalytic performance under continuous operating conditions is further examined by chronoamperometric measurements. Fig. S10† shows the current–time curves recorded at −0.23 V for 1800 s. The Pd NS catalysts maintain a stable current density of 0.64 mA cm^{-2}, which is about 2.5 times higher than that of commercial Pd/C; the Pd CNs also exhibit a higher current density than Pd/C, demonstrating again the significantly enhanced electrocatalytic activity and stability of our prepared Pd NCs.

Conclusion

In summary, we propose a facile, rapid, and efficient route to synthesize well-defined and high yield Pd NSs and CNs in aqueous solution without using any organic solvents and surfactants as protecting and structure-directing agents, ensuring the as-made Pd NCs have a definitely "clean" surface, allowing them to exhibit a high activity for methanol oxidation. These encouraging findings would certainly assist the long-term endeavours to further enhance the catalytic activity of PGMs. Besides, as catalysts, these NPs could be used in broad fields including optical, magnetic, and electrical applications.

Acknowledgements

The authors thank Prof. Wei Xing for the help in the electrochemical experiment. This work is financially supported by 100 Talents Programme of The Chinese Academy of Sciences, the Foundation for Innovative Research Groups of the National Natural Science Foundation of China (no. 20921002), National Natural Science Foundation of China (Grant no. 21101147), and the Jilin Province Science and Technology Development Program (Grant no. 20100102 and 20116008).

References

1 (*a*) Z. Chen, Z. M. Cui, F. Niu, L. Jiang and W. G. Song, *Chem. Commun.*, 2010, **46**, 6524; (*b*) N. Tian, Z. Zhou and S. Sun, *Chem. Commun.*, 2009, 1502; (*c*) X. Yu, D. Wang, Q. Peng and Y. Li, *Chem. Commun.*, 2011, **47**, 8094; (*d*) Y. Liu, M. Chi and S. H. Sun, *Chem. Mater.*, 2011, **23**, 4199; (*e*) H. Lee, S. Habas and P. Yang, *Angew. Chem., Int. Ed.*, 2006, **45**, 7824.
2 (*a*) X. M. Chen, G. H. Wu, J. M. Chen, X. Chen, Z. X. Xie and X. Wang, *J. Am. Chem. Soc.*, 2011, **133**, 3693; (*b*) Z. H. Zhang, J. J. Ge, L. Ma, J. H. Liao, T. H. Lu and W. Xing, *Fuel Cells*, 2009, **2**, 114; (*c*) J. Ge, W. Xing, X. Xue, C. Liu, T. Lu and J. Liao, *J. Phys. Chem. C*, 2007, **111**, 17305.
3 (*a*) L. G. Feng, X. J. Sun, C. P. Liu and W. Xing, *Chem. Commun.*, 2012, **48**, 419; (*b*) Z. Y. Zhou, X. Kang, Y. Song and S. Chen, *Chem. Commun.*, 2011, **47**, 6075.
4 (*a*) C. Bianchini and P. K. Shen, *Chem. Rev.*, 2009, **109**, 4183; (*b*) R. Schennach, A. Eichler and K. D. Rendulic, *J. Phys. Chem. B*, 2003, **107**, 2552; (*c*) F. Z. Si, L. Ma, X. B. Zhang and W. Xing, *RSC Adv.*, 2012, **2**, 401.
5 (*a*) A. M. Cao, R. Lu and G. Veser, *Phys. Chem. Chem. Phys.*, 2010, **12**, 13499; (*b*) A. Mohanty, N. Garg and R. Jin, *Angew. Chem., Int. Ed.*, 2010, **49**, 1; (*c*) R. Narayanan and M. A. El-Sayed, *J. Am. Chem. Soc.*, 2004, **126**, 7194; (*d*) M. Subhramannia and V. K. Pillai, *J. Mater. Chem.*, 2008, **18**, 5858.
6 (*a*) Z. Y. Zhou, N. Tian, J. T. Li, I. Broadwell and S. G. Sun, *Chem. Soc. Rev.*, 2011, **40**, 4167; (*b*) T. K. Sau and A. L. Rogach, *Adv. Mater.*, 2010, **22**, 1781.
7 (*a*) M. S. Jin, H. Zhang, Z. X. Xie and Y. Xia, *Angew. Chem., Int. Ed.*, 2011, **50**, 1; (*b*) Y. Xiong, J. McLellan, J. Chen, Y. Yin, Z. Li and Y. Xia, *J. Am. Chem. Soc.*, 2005, **127**, 17118; (*c*) B. Lim, Y. Xiong and Y. Xia, *Angew. Chem.*, 2007, **119**, 9439; (*d*) Y. Xiong, H. Cai, B. Wiley, J. Wang, M. Kim and Y. Xia, *J. Am. Chem. Soc.*, 2007, **129**, 3665; (*e*) Y. Ding, F. Fan, Z. Tian and Z. L. Wang, *J. Am. Chem. Soc.*, 2010, **132**, 12480.
8 (*a*) M. P. Pileni, *Nat. Mater.*, 2003, **2**, 145; (*b*) B. S. Fu, M. N. Missaghi, C. M. Downing, M. C. Kung, H. H. Kung and G. M. Xiao, *Chem. Mater.*, 2010, **22**, 2181; (*c*) O. M. Wilson, R. W. J. Scott, J. C. Garcia-Martinez and R. M. Crooks, *J. Am. Chem. Soc.*, 2005, **127**, 1015.
9 J. A. Lopez-Sanchez, N. Dimitratos and G. J. Hutchings, *Nat. Chem.*, 2011, **3**, 551.
10 A. Chernov, *Sov. Phys. Crystallogr.*, 1972, **16**, 734.
11 (*a*) J. Park, B. Koo, Y. Hwang, C. Bae, K. An, J. G. Park, H. M. Park and T. Hyeon, *Angew. Chem.*, 2004, **116**, 2332; (*b*) B. Koo, J. Park, Y. Kim, S. H. Choi, Y. E. Sung and T. Hyeon, *J. Phys. Chem. B*, 2006, **110**, 24318; (*c*) T. Yu, D. Y. Kim, H. Zhang and Y. Xia, *Angew. Chem., Int. Ed.*, 2011, **50**, 1.